Volume 1 | Number 1 | Jan 2013 | Pages 1–100

Polymer Chemistry

www.rsc.org/polymers

ROYAL SOCIETY OF CHEMISTRY

www.rsc.org/polymers

Polymer Chemistry

ROYAL SOCIETY OF CHEMISTRY

Polymer Chemistry

ARTICLE

Controlled Release of an Anti-Cancer Drug-Paclitaxel by Using Nano-Structured Amphiphilic Star-Hyperbranched Block copolymers

Caner Geyik,[a] Mustafa Ciftci,[b] Bilal Demir,[c] Bahar Guler,[c] A. Burak Ozkaya,[d] Z. Pınar Gumus,[a] F. Baris Barlas,[c] Dilek Odaci Demirkol,[c*] Hakan Coskunol,[a] Suna Timur,[a,c] and Yusuf Yagci[b*]

In the present study, two amphiphilic star-hyperbranched copolymers, poly(methyl methacrylate)-*b*-poly(2-hydroxyethyl methacrylate) (PMMA-*b*-PHEMA), with different hydrophilic PHEMA segment content (PMMA-*b*-PHEMA-1, and PMMA-*b*-PHEMA-2) were synthesized and their drug loading and release profiles were examined by using paclitaxel (PTX) as a model drug. Drug loading capacity and encapsulation efficiency were found to be similar in both polymers. Encapsulation efficiency found to be prominent with 98% and 98.5% for PMMA-*b*-PHEMA-1 and PMMA-*b*-PHEMA-2, respectively. On the other hand, drug release behaviors were varied in favor of the block copolymer comprising shorter PHEMA chains (PMMA-*b*-PHEMA-1). Additionally, to assess biological effects of PTX-loaded polymers, human non-small cell lung carcinoma (A549) cells were used. Cell viability and cell cycle analysis showed that both polymers were not toxic to the cells. Cytotoxic effects of PTX-loaded PMMA-*b*-PHEMA-1 on A 549 cells were higher (66.49% cell viability at 5.0 ng/mL PTX) than that of PMMA-*b*-PHEMA-2 (72.47% cell viability at 5.0 ng/mL PTX) consistent with the drug release experiments.

1. Introduction

Cancers are among major diseases with high morbidity and mortality rate worldwide, especially in advanced countries due to prolonged lifetime[1]. Therefore, enormous amount of research has been carried out for decades to address this disease. However, all of the current strategies dealing with this problem including dissection, chemotherapy, and radiotherapy have limitations[2]. Thus, development of new methods and modification of current methods have emerged. One of the major breakthroughs of the cancer targeted drug research was the discovery of "enhanced permeability and retention" (EPR) effect, first reported by Matsumura and Maeda[3]. EPR effect describes an increase in the permeability of tumor supplying blood vessels due to structural defects. Therefore, molecules having long-circulating properties such as biocompatible nanoparticles[4], liposomes[5], and amphiphilic micelles[6,7] tend to accumulate in solid tumors *via* EPR effect[8–10]. Another important characteristic that a carrier should bear is to be responsive to cancerous environment or external stimuli in a

way that the drug of interest could be released at the tumor site instead of healthy tissues.

Among the macromolecules used for drug delivery, hyperbranched polymeric micelles are of great interest owing to their unique structures, in which the hydrophobic core encapsulates the poorly water-soluble therapeutic agent and the hydrophilic outer surface plays as a stabilizing interface between the core and physiological media[11,12]. Their controllable size distributions also make it possible to obtain macromolecules small enough to penetrate vascular defects of solid tumor as well as large enough to prevent renal clarification permitting longer bioavailability[10,13]. Besides, they are suitable to be further modified for targeting and/or imaging purposes[14,15,16,17]. In our previous study, we have shown that PMMA-*b*-PHEMA micelles can further be modified with arginylglycylaspactic acid (RGD) and **T**rans-**A**ctivator of **T**ranscription (TAT) peptide to enhance cell selectivity and membrane penetration properties[7]which is similar to peptide modified conducting polymer structures in the field of bio-based covering materials[18,19]. It is not surprising to see the reflection of the properties mentioned above in development of novel drugs by pharmaceutical companies, some of which are advanced to Phase I and Phase II clinical trial stages[20].

Paclitaxel (PTX), a chemotherapeutic agent derived from the bark of the Western Yew tree[21], was demonstrated to be effective against several cancer cell lines *in vitro*[22,23]. Early studies have determined the main anticancer effect of PTX as the disruption of the microtubule depolymerization[24], which is crucial for mitotic spindle formation[25]. Thus, a blockage in the spindle formation results in cell cycle arrest in mitosis (M)

[a.] Ege University, Institute on Drug Abuse, Toxicology and Pharmaceutical Sciences, 35100, Izmir/TURKEY.
[b.] Istanbul Technical University, Department of Chemistry, 34469, Istanbul/TURKEY. E-mail: yusuf@itu.edu.tr
[c.] Ege University, Faculty of Science, Department of Biochemistry, 35100, Izmir/TURKEY. E-mail: dilek.demirkol@yahoo.com
[d.] Ege University, School of Medicine, Department of Medical Biochemistry, 35100, Izmir/TURKEY
† Electronic Supplementary Information (ESI) available: ¹H NMR and FT-IR spectra, Particle Size and TEM analysis. See DOI: 10.1039/x0xx00000x

Polymer Chemistry Accepted Manuscript

phase[26,27]. However, later studies showed that, the effect of PTX to be concentration dependent and mechanisms other than microtubule depolymerization play role in anticancer properties of this drug[28,29].

In this study, two amphiphilic star-hyperbranched copolymers, namely poly(methyl methacrylate)-*b*-poly(2-hydroxyethyl methacrylate) (PMMA-*b*-PHEMA), with different PHEMA chain length exhibiting different hydrophilic character have been compared as potential drug carriers. Polymers were synthesized by two-step process and characterized by NMR, FT-IR, and size exclusion chromatography. Drug loading properties and drug release profiles by using PTX as a model drug were evaluated. Additionally, biological effects on human non-small cell lung carcinoma cells were assessed with MTT cell viability assay and cell cycle analysis via flow cytometry.

2. Experimental Section

Materials. Commercial paclitaxel (PTX) solution (Anzatax Injection) containing 30 mg/5.0 mL drug was used. Dulbecco's Modified Eagle Medium (DMEM), Penicillin/Streptomycin (10,000 UI/mL), L-Glutamine (200 mM). Trypsin/EDTA (0.05% Trypsin; 0.20 g/L EDTA), and Phosphate Buffered Saline (PBS) used in cell culture experiments were purchased from LONZA. Fetal Bovine Serum (FBS) was obtained from BIOWEST. Dimethyl sulfoxide (DMSO), 3-(4,5-dimethylthiazolyl-2)-2,5-diphenyltetrazolium bromide (MTT), and sodium dodecyl sulfate (SDS) were purchased from SIGMA. Cycletest™ Plus DNA Reagent Kit (BD BIOSCIENCES) was used for cell cycle analysis by flow cytometry.

Methyl methacrylate (MMA, 99%; Aldrich) and and 2-hydroxyethyl methacrylate (HEMA, 99%, Aldrich) were passed through a basic alumina column to remove the inhibitor. 2-Bromoethyl methacrylate (2-BEMA) was kindly donated by Bicak research group. Dimanganese decacarbonyl ($Mn_2(CO)_{10}$, 99%, Aldrich) was purified by sublimation and stored in a refrigerator in the dark. *n*-Hexane (95%, Aldrich), anhydrous N,N-dimethylformamide (DMF, 99.8%, Aldrich), tetrahydrofuran (THF, ≥99%, Aldrich) and methanol (MeOH; 99.9%, Merck) were used as received.

Characterization of polymers. ^{1}H NMR spectra of the polymers were recorded on an Agilent VNMRS 500. FT-IR analyses were performed on a Perkin-Elmer FT-IR Spectrum One B spectrometer.

Size exclusion chromatography (SEC) measurements were obtained from a Shimadzu Co. system. SGX (100 Å and 7 nm diameter loading material) 3.3 mm i.d. × 300 mm column, was used for the DMF eluent at 25°C (flow rate: 0.4 mL.min^{-1}). The detectors were calibrated with polystyrene standards having narrow molecular weight distribution.

The ratio between $M_{n,RI}$ and $M_{n,LS}$ (RM = $M_{n,RI}/M_{n,LS}$) gives qualitative information about the branching density of the polymers since branched structures are more compact than linear polymers for a given molecular weight[30]. As can be seen in Table 1, the R_M value significantly differs as polymer

architecture moves from lightly branched (R_M=0.32) to highly branched architectures (R_M=0.23). This parameter thus indicates a trend of branching density of the synthesized polymers.

Synthesis of PMMA-*b*-PHEMA. PMMA-*b*-PHEMA copolymers were prepared by a two-step process. A representative photopolymerization procedure is as follows: In the first step, bromo functional hyperbranched PMMA macroinitiator was synthesized by radicalic photopolymerization of MMA and 2-BEMA as described previously[31]. Then, the obtained macroinitiator, (250 mg, 6.3 x 10^{-6} mol), $Mn_2(CO)_{10}$ (20.8 mg, 5.3 x10^{-5} mol), HEMA (2.0 mL, 1.5x10^{-2} mol) and 2.0 mL of DMF were placed in a Pyrex tube equipped with a magnetic stirring bar and filled with dry nitrogen. The mixture was irradiated by a Ker-Vis blue photoreactor equipped with six lamps (Philips TL-D 18 W) emitting light nominally at 400– 500 nm at room temperature. At the end of irradiation, the copolymer was precipitated in *n*-hexane and characterized by ^{1}H-NMR, FT-IR and GPC measurements.

Preparation of PTX-loaded polymers. 1.0 mg of the polymer (PMMA-*b*-PHEMA-1 or PMMA-*b*-PHEMA-2) was dissolved in DMSO in a water bath sonicator. 250 μL of the 1.0 mg/mL polymer solution and 41.67 μL of 6.0 mg/mL PTX solution were mixed, and PBS (pH 7.4) was added to make a final volume of 1.0 mL. The resultant polymer-PTX solution was incubated for 24 h at 1000 rpm and 24 ^{o}C to accomplish the efficient PTX encapsulation. Following the drug loading process, the solution was centrifuged through 10 kDa filters for three times with PBS to remove free PTX and final solution was completed to 1.0 mL with PBS. Obtained solution was used for further characterization and *in vitro* cell culture experiments.

Drug Loading Capacity and Encapsulation Efficiency. The encapsulation efficiency (EE) and drug loading (DL) were calculated according to following equations as described elsewhere [32,33].

$$DL\ (\%) = \frac{\left[\begin{smallmatrix}Weight\ of\\Feeding\ PTX\end{smallmatrix}\right]-\left[\begin{smallmatrix}Weight\ of\\unincorporated\ PTX\end{smallmatrix}\right]}{\left[\begin{smallmatrix}Weight\ of\\Feeding\ polymer\ and\ PTX\end{smallmatrix}\right]} \quad \text{(Eq. 1)}$$

$$EE\ (\%) = \frac{\left[\begin{smallmatrix}Weight\ of\\Feeding\ PTX\end{smallmatrix}\right]-\left[\begin{smallmatrix}Weight\ of\\unincorporated\ PTX\end{smallmatrix}\right]}{\left[\begin{smallmatrix}Weight\ of\\Feeding\ PTX\end{smallmatrix}\right]} \quad \text{(Eq. 2)}$$

To determine the DL and EE (%), the PTX amounts in rinsed water (for both PMMA-*b*-PHEMA-1 and PMMA-*b*-PHEMA-2) were analyzed *via* high-performance liquid chromatography (HPLC). An Agilent HPLC system with DAD detector at a wavelength of 227 nm was used for the detection of PTX. A C18 column was used at 25 ^{o}C (Agilent Eclipse column XDB-C18, 5.0 μm particle size, 4.6x150 mm) for the analysis. The mobile phase consisted of ultra-pure water (1.0% phosphoric acid) and acetonitrile (40:60, v:v). The flow rate was 1.2 mL/min and injection volume was 20 μL for each sample. Limit

of detection (LOD) and limit of qualification (LOQ) were calculated as 1.91 ng/mL and 6.36 ng/mL, respectively. PTX amounts in the rinsing buffer were detected by comparing the peak areas with the standard curve.

Physicochemical characterization of PTX-loaded polymers. Particle size and polydispersity of the PTX-loaded polymers were assessed by dynamic light scattering (DLS) (Zetasizer Nano ZS, Malvern Instruments Ltd.) with 90° scattering angle at 633 nm. Measurements were performed at 25 ^{o}C in triplicate.

The morphological structure of the PTX-loaded PMMA-*b*-PHEMA-1 was investigated by transmission electron microscopy (TEM, FEI Tecnai G^2 Spirit BioTwin,) with a 120 kV.

In vitro release of PTX-loaded polymers. *In vitro* release behavior of PTX-loaded polymers was monitored by creating artificial media. pH 7.4 and pH 6.0 (PBS) were used to simulate the healthy and cancerous cellular environment, respectively. Dialysis bags containing 1.0 mL of sample were submerged into 20 mL buffer medium at 37 ^{o}C at 100 rpm. To investigate *in vitro* release profiles of samples, 1.0 mL of the samples was collected at several time intervals (0, 30 min and 1, 2, 4, 6, 8, 12, 24, 48, 72 h) and replaced with an equal volume of fresh medium. The concentration of PTX in collected samples was determined by HPLC (as described above) with correction for volume replacement. Equivalent PTX concentration to encapsulated PTX in polymers was used as control. Probing the released PTX, cumulative drug release percent (E_r) was calculated according to the following equation[34]:

$$\mathrm{Er} = \frac{Ve \sum_1^{n-1} Ci + Vo\, Cn}{M(PTX)}$$

where $M(PTX)$ represents the amount of PTX in the polymers, Vo is the whole volume of the release media (Vo = 20 mL), Ve is the volume of the replace media (Ve = 1.0 mL), and Cn represents the concentration of PTX in the nth sample. Three groups of replicate measurements were carried out for each time point.

Cell culture. Human non-small cell lung carcinoma cell line, A549 (American Type Culture Collection, ATCC), was maintained in DMEM supplemented with 10% FBS, 100 UI/mL Penicillin/Streptomycin, and 2.0 mM L-Glutamine at 37°C in a humidified incubator with 5.0% CO_2. All cells were sub-cultured at 80% confluency by trypsinization every two or three days.

Cell viability. Cell viability was determined by mitochondrial oxidoreductase activity of living cells after incubating the cells with various concentrations of tested materials. Colorimetric MTT assay was used to assess relative cell viability. Briefly, 10,000 A549 cells/well were incubated in 96-well cell culture plate for 24 h at standard culture conditions. After the incubation, cells were treated either with PTX containing

solutions (PTX, PMMA-*b*-PHEMA-1/PTX, and PMMA-*b*-PHEMA-2/PTX) or polymers alone for 72 h. All solutions were prepared in DMEM with final PTX or polymer concentrations of 0.10, 0.50, 1.0, 5.0, 10, 50, and 100 ng/mL. MTT solution (0.5 mg/mL in DMEM) was added to each well and incubated for 4 h. Intracellular formazan crystals produced by the enzymatic activity of living cells were dissolved in 10% SDS (overnight) and quantified by reading the absorbance at 570 nm. Absorbance at 620 nm was used as reference wavelength. DMEM without any sample was used as control and considered as 100% viable. Relative cell viability was plotted as the percent absorbance of sample treated cells (n=6). Statistical comparison of the effects of PTX and PTX-loaded polymers (PMMA-*b*-PHEMA-1 and PMMA-*b*-PHEMA-2) on cell viability was performed by non-parametric Mann-Whitney U test (GraphPad Software v5.02).

Cell cycle analysis by flow cytometry. 200,000 A549 cells/well were incubated in 6-well cell culture plate for 24 h. Cells were pre-incubated for 24h with FBS-free DMEM to synchronize cell cycle. Following serum starvation, cells were incubated with PTX, PMMA-*b*-PHEMA-1/PTX, PMMA-*b*-PHEMA-2/PTX (equivalent PTX concentration of 5.0 ng/mL), PMMA-*b*-PHEMA-1, and PMMA-*b*-PHEMA-2 (5.0 ng/mL, the same concentration with representative conjugate) for 12 h. Cells were prepared for the flow cytometry analysis as recommended in manufacturer's protocol. 20,000 cells were analyzed for propidium iodide (PI) fluorescence signal in flow cytometer (FACSAria, BD BIOSCIENCES). Data were plotted by using Flowing Software 2.5.1 (Cell Imaging Core, Turku Centre for Biotechnology).

3. Results and Discussion

Synthesis and characterization of amphiphilic star-hyperbranched copolymer. Star-hyperbranched PMMA-*b*-PHEMA copolymers were obtained by two discrete steps. In the first step, a bromo functional hyperbranched poly(methyl methacrylate) (PMMA) hydrophobic core was prepared by $Mn_2(CO)_{10}$ based self-condensing vinyl polymerization (SCVP) of methyl methacrylate (MMA) with 2-bromoethyl methacrylate (BEMA). As consequence of the process, some of the bromine groups of BEMA are not activated and thus the resulting hyperbranched polymers contain a fraction of bromine groups in the structure which allows further polymerization. Thus, visible light induced polymerization of HEMA initiated by the photolysis of $Mn_2(CO)_{10}$ in the presence of the obtained macroinitiators resulted in the formation of the amphiphilic PMMA-*b*-PHEMA copolymers possessing hydrophobic hyperbranched core and hydrophilic chains (Scheme 1).
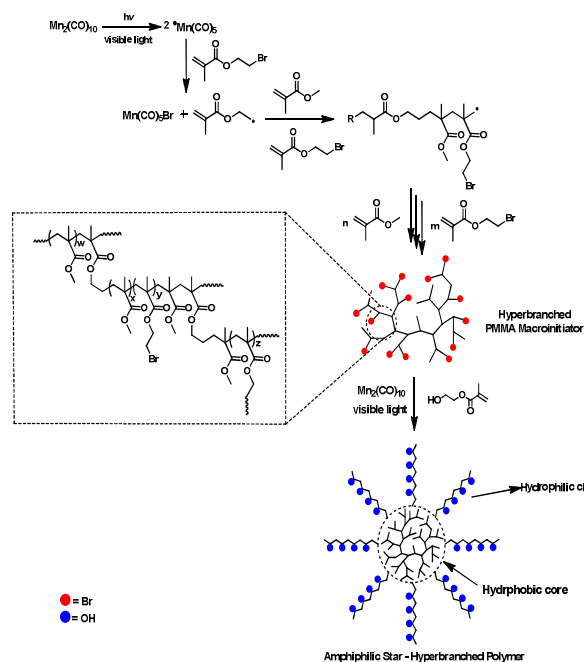
Scheme 1. Synthesis of amphiphilic star-hyperbranched PMMA-*b*-PHEMA block copolymer by combination of SCVP and visible light-induced free radical polymerization.

Table 1. Synthesis of the amphiphilic star-hyperbranched copolymers by photocopolymerization of bromo functional hyperbranched PMMA macroinitiator[a] with HEMA in the presence of $Mn_2(CO)_{10}$.

Polymer	Time (h)	Conv. [%][b]	Mn, RI g/mol[c]	Mn, LS g/mol[d]	RM
PMMA-b-PHEMA-1	3	36	22,310	78,310	0.28
PMMA-b-PHEMA-2	8	79	447,100	186,290	0.23

[a]$M_{n,RI}$: 12 690 g/mol, $M_{n,LS}$: 39 670 g/mol, R_M: 0,32 [b]Determined gravimetrically. [c]With refractive index detector. [d]With light scattering detector.

As can be seen from Table 1, the molecular weight and the branching density of the copolymers increase with the irradiation time. Since the same macroinitiator was used in both cases, the higher molecular weight might be attributed to prolonged irradiation time resulting in longer outer sphere linear PHEMA chain growth.

The structure of the precursor polymer and the final star block copolymers was confirmed by ^1H NMR analysis. The NMR spectrum of the block copolymer, PMMA-*b*-PHEMA-1 displays signals at 3.5–4.4 ppm region corresponding to −CH_2O, −OCHH_2, and −OH protons of PHEMA segments, in addition to the characteristic bands of the PMMA core (Figure S1).

The results obtained from FT-IR spectroscopy also support the successful block copolymerization. The IR-spectra of the block copolymers exhibit the OH stretching band of PHEMA star arms in addition to characteristic bands of PMMA core (Figure S2).

Drug loading capacity and encapsulation efficiency. Drug loading and encapsulation efficiency are important parameters

to evaluate the properties of the drug carrier systems. Drug loading and encapsulation characteristics of the PMMA-*b*-PHEMA-1 and PMMA-*b*-PHEMA-2 block copolymers were calculated according to the Eq. (1) and Eq. (2). Prior to injection of unincorporated PTX solution, a calibration curve with various PTX concentrations (10–500 ng/mL) *versus* integrated area was drawn with the equation of y = 0.044x+0.347, and a correlation coefficient of 0.9998. As shown in the Table 2, PTX loading and EE (%) for both PMMA-*b*-PHEMA block copolymers achieved about the maximum limits. The DL (%) and EE (%) for the PTX-loaded PMMA-*b*-PHEMA-1, the DL (%) and EE (%) were 46.0 and 98.0, respectively. The corresponding values for PTX-loaded PMMA-*b*-PHEMA-2 were 46.25 and 98.5. Despite the fact that PMMA-*b*-PHEMA-1 has higher hydrophobicity both hyper-branched copolymer structure presented similar DL and EE characteristics. This result also indicates that PMMA hydrophobic cores of these polymers created greater cavities for the encapsulation of PTX. As a consequence, DL of these polymers were higher when compared to the other PTX-loaded polymeric micelles such as AB block copolymer of poly(N-(2-hydroxypropyl) methacrylamide lactate) and poly(ethylene glycol) (22.0 wt%)[35], poly(lactic acid)-poly(ethylene glycol (25.0 wt%)[36] and octyl modified serum albumin (33.1 wt%)[33].

Table 2. Drug loading capacity, encapsulation efficiency and particle size results of the PTX-loaded amphiphilic hyperbranched polymers.

	DL (%)	EE (%)	Particle Size (nm ± S.D.)[a]	PDI[b]
PMMA-*b*-PHEMA-1/PTX	46	98	21.42±4.22	0.345
PMMA-*b*-PHEMA-2/PTX	46.25	98.5	18.92±2.31	0.476
PMMA-*b*-PHEMA-1	-	-	19.6±3.4	0.317
PMMA-*b*-PHEMA-2	-	-	24.7±5.00	0.478

[a] S.D. standard deviation

Physicochemical characteristics of PTX-loaded polymers. In this work, PTX were introduced into PTX-loaded PMMA-*b*-PHEMA-1 and PTX-loaded PMMA-*b*-PHEMA-2 which are amphiphilic hyperbranched polymers. After the determination of DL and EE properties of the polymers, they were characterized using dynamic light scattering. The hydrodynamic diameters of PTX-loaded polymers were presented in Table 2. From the particle size analysis, hydrodynamic diameters of both PTX-loaded polymers were 21.42 and 18.92 nm, respectively. The sizes of unloaded polymers were also determined as 19.6 nm and 24.5 nm for PMMA-*b*-PHEMA-1 and PMMA-*b*-PHEMA-2, respectively. Moreover, the hydrodynamic particle size was investigated in both pH 7.4 and 6.0 PBS. Notably, no dramatic change was observed for both polymers at different pH conditions (Figure S3).

PTX-loaded PMMA-*b*-PHEMA-1 was further characterized by TEM which showed the particles smaller than 50 nm in size. (Figure S4).

In vitro release profiles of PTX-loaded polymers. In addition to the characterization steps, *in vitro* release profiles of PTX-loaded polymers were generated in order to investigate the potential use of these amphiphilic star-hyperbranched polymers as delivery carriers. Figure 1 demonstrates the comprehensive PTX release of free and polymer-encapsulated PTX at different pH values. Both polymers presented an increased PTX release in acidic conditions (Fig. 1A and B). This is an important issue since extracellular pH of cancer cells are lower compare to that of the healthy tissues[37]. Owing to the characteristics of the polymers presented, higher drug release could occur in solid tumor tissues, ensuing lower side effects.

When the cumulative release graphics of two polymers were compared, PTX release from PMMA-*b*-PHEMA-1 was higher than PMMA-*b*-PHEMA-2 in both experimental settings. Moreover, a sustained release of PTX was observed when PMMA-*b*-PHEMA-1 was used as drug carrier in pH 6.0 which simulates the pH of tumor microenvironment[38]. As a result, practically constant PTX doses were achieved. This feature may have a particular importance in case of fast metabolized drugs[39]. When compared to PMMA-*b*-PHEMA-1, PMMA-*b*-PHEMA-2 seems to prevent drug release up to 72 h at both pH 7.4 and 6.0, before exhibiting an exponential increase in drug release. Differences between drug release profiles of the polymers can be attributed to varying hydrophilic chain lengths since both polymers share the same hydrophobic core. Longer hydrophilic chains presented in PMMA-*b*-PHEMA-2 can increase the impedance of the diffusion of hydrophobic PTX[40]. Accordingly, PMMA-*b*-PHEMA-1 could exhibit a higher drug release up to 83% in pH 6.0, whereas PMMA-*b*-PHEMA-2 resumed its PTX release around 66%. On the other hand, PMMA-*b*-PHEMA-1 demonstrates higher drug release as 30%, and a similar drug release study with amphiphilic star-shaped polymers showed approximately same value at pH between 7.4 and 5.3[41]
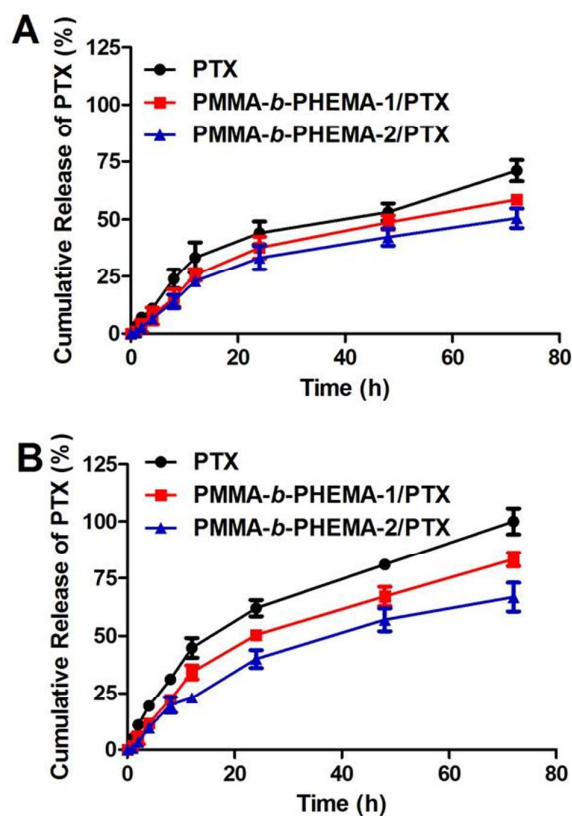

Figure 1. *In vitro* release behavior of PTX-loaded polymers at pH 7.4 (A) and 6.0 (B), (37 ^{o}C, 100 rpm).

Effects of the polymers and PTX-loaded polymer conjugates on cell viability. Polymers used in this study showed no significant effect on cell viability (Fig. 2A). PTX alone showed inhibitory effects on cell viability at doses 5.0 ng/mL and above (Fig. 2B), as well as PTX-loaded polymer conjugates (Fig. 2B). However, cytotoxic effects of PTX found to be lower when it is loaded to carrier polymers. At 5.0 ng/mL, relative cell viability of PTX treated cells was 55.88%, whereas relative cell viabilities of PTX-loaded PMMA-*b*-PHEMA-1/PTX and PTX-loaded PMMA-*b*-PHEMA-2/PTX treated cells were found 66.49% (p= 0.005) and 72.47% (p= 0.002), respectively. This is an expected result as both polymers release the drug in time dependent manner and thus, PTX concentrations were lower compared to free PTX. This data is consistent with the drug release experiments, where PMMA-*b*-PHEMA-1/PTX releases PTX in higher amounts compared to PMMA-*b*-PHEMA-2/PTX (vide ante).
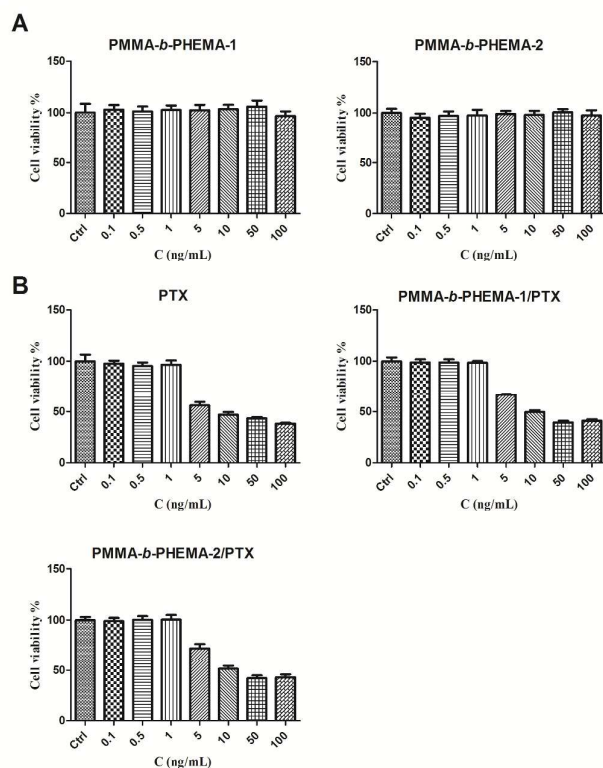
Figure 2. The effects of the samples on cell viability after 72 h exposure (MTT assay was used). A) PMMA-*b*-PHEMA-1 and PMMA-*b*-PHEMA-2 alone. B) PTX, PTX-loaded PMMA-*b*-PHEMA-1, and PTX-loaded PMMA-*b*-PHEMA-2, [Ctrl: Control, *n*=6].

Cell cycle analysis. To further investigate the effects of PTX compared to PTX-loaded polymers, analysis of cell cycle was carried out (Fig. 3). Both polymers showed similar cell cycle progression compared to non-treated controls. On the other hand, PTX and PTX-loaded polymers resulted in a substantial accumulation of sub-G1 cell population, which indicates apoptosis in A549 cells. Given the main mechanism of action of PTX is inhibition of the spindle formation, an increase in G2/M peak would be expected. However, PTX induced cell cycle arrest in M phase requires higher concentrations [28,29,42]. Therefore, an increase in sub-G1 rather than G2/M arrest occurred in PTX treated cells.

Observed sub-G1 cell population was lower in PTX-loaded polymer conjugates compared to PTX alone (Table 3). This is complementary to drug release and cell viability studies, in which the release of PTX from polymers was lower than free PTX. Among the conjugates used, PTX-loaded PMMA-*b*-PHEMA-1/PTX resulted in higher sub-G1 peak as a result of increased PTX release owing to its shorter hydrophilic arms.

Table 3. Apoptotic cell ratio calculated from flow cytometric sub-G1 populations

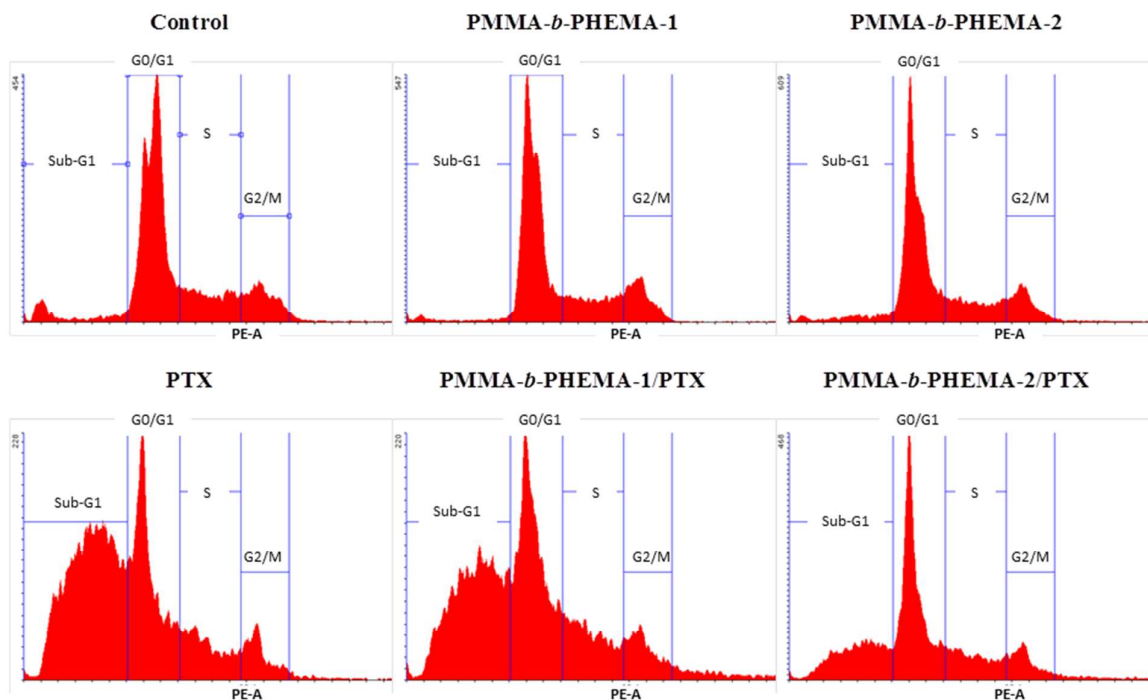|	Control	PMMA-b-PHEMA-1	PMMA-b-PHEMA-2	PTX	PMMA-b-PHEMA-1/PTX	PMMA-b-PHEMA-2/PTX
Apoptotic Cells (%)	7.11	3.62	6.99	51.46	38.77	25.43

Figure 3. Flow cytometric analyses for cell cycle progression. Apoptotic cell population was shown as Sub-G1 peak. PTX-loaded PMMA-*b*-PHEMA-1 and PTX-loaded PMMA-*b*-PHEMA-2 have shown similar profile compared to control group. PTX and PTX-loaded polymers, induced apoptosis after 12 h of treatment, (PTX: Paclitaxel)

Conclusions

In summary, two amphiphilic hyperbranched polymers with different hydrophilic side chains were synthesized and compared as potential drug carriers. Model chemotherapeutic PTX was successfully encapsulated to carrier polymers with encapsulation efficiencies above 98%. Drug release profiles as well as their effects on human non-small cell lung carcinoma cells were examined. Both polymers showed PTX release in a time dependent manner. Besides, release of PTX was pH dependent, which was in favor for acidic environment. This is mainly important because of the acidic environment present in the extracellular matrix of solid tumors. In aqueous media, PTX-loaded PMMA-*b*-PHEMA-1, bearing short hydrophilic side chain, showed higher drug release up to 72 h. Similarly, PTX-loaded PMMA-*b*-PHEMA-1 resulted in higher inhibition of cell viability as well as higher induction in sub-G1 peak which is associated with apoptosis. These results demonstrate the importance of the micelle structure in terms of drug release properties. Additionally, proposed carrier systems might also be used for imaging and/or targeting studies with further modification with fluorescent dyes, antibodies or aptamers.

Acknowledgements

Notes and references

1   B. W. Stewart and C. P. Wild, *World Cancer Report 2014*, 2014.
2   J. Fang, H. Nakamura and H. Maeda, *Adv. Drug Deliv. Rev.*, 2011, **63**, 136–51.
3   Y. Matsumura and H. Maeda, *Cancer Res.*, 1986, **46**, 6387–92.
4   M. Kumagai, T. K. Sarma, H. Cabral, S. Kaida, M. Sekino, N. Herlambang, K. Osada, M. R. Kano, N. Nishiyama and K. Kataoka, *Macromol. Rapid Commun.*, 2010, **31**, 1521–8.
5   M. H. Li, H. Yu, T. F. Wang, N. D. Chang, J. Q. Zhang, D. Du, M. F. Liu, S. L. Sun, R. Wang, H. Q. Tao, S. L. Geng, Z. Y. Shen, Q. Wang and H. S. Peng, *J. Mater. Chem. B*, 2014, **2**, 1619.
6   H. Dong, N. Dube, J. Y. Shu, J. W. Seo, L. M. Mahakian, K. W. Ferrara and T. Xu, *ACS Nano*, 2012, **6**, 5320–9.
7   M. Seleci, D. A. Seleci, M. Ciftci, D. Odaci Demirkol, F. Stahl, S. Timur, T. Scheper and Y. Yagci, *Langmuir*, 2015.
8   J. Gallo, N. J. Long and E. O. Aboagye, *Chem. Soc. Rev.*, 2013, **42**, 7816–33.
9   M. Nakayama and T. Okano, *React. Funct. Polym.*, 2011, **71**, 235–244.
10 V. Torchilin, *Adv. Drug Deliv. Rev.*, 2011, **63**, 131–5.
11 J.-Z. Du, L.-Y. Tang, W.-J. Song, Y. Shi and J. Wang, *Biomacromolecules*, 2009, **10**, 2169–74.
12 S. Vandewalle, S. Wallyn, S. Chattopadhyay, C. R. Becer and F. Du Prez, *Eur. Polym. J.*, 2015.
13 V. P. Torchilin, *J. Control. Release*, 2001, **73**, 137–172.
14 S. Chen, X.-Z. Zhang, S.-X. Cheng, R.-X. Zhuo and Z.-W. Gu, *Biomacromolecules*, 2008, **9**, 2578–85.
15 D. J. Coles, B. E. Rolfe, N. R. B. Boase, R. N. Veedu and K. J. Thurecht, *Chem. Commun. (Camb).*, 2013, **49**, 3836–8.
16 Q. Zhang, L. Su, J. Collins, G. Chen, R. Wallis, D. A. Mitchell, D. M. Haddleton and C. R. Becer, *J. Am. Chem. Soc.*, 2014, **136**, 4325–32.
17 I. Kurtulus, G. Yilmaz, M. Ucuncu, M. Emrullahoglu, C. R. Becer and V. Bulmus, *Polym. Chem.*, 2014, **5**, 1593–1604.
18 H. Akbulut, M. Yavuz, E. Guler, D. O. Demirkol, T. Endo, S. Yamada, S. Timur and Y. Yagci, *Polym. Chem.*, 2014, **5**, 3929.
19 M. Kesik, H. Akbulut, S. Söylemez, Ş. C. Cevher, G. Hızalan, Y. Arslan Udum, T. Endo, S. Yamada, A. Çırpan, Y. Yağcı and L. Toppare, *Polym. Chem.*, 2014, **5**, 6295–6306.
20 M. J. Vicent, H. Ringsdorf and R. Duncan, *Adv. Drug Deliv. Rev.*, 2009, **61**, 1117–20.
21 M. C. Wani, H. L. Taylor, M. E. Wall, P. Coggon and A. T. McPhail, *J. Am. Chem. Soc.*, 1971, **93**, 2325–7.
22 2Y. H. Choi and Y. H. Yoo, *Oncol. Rep.*, 2012, **28**, 2163–9.
23 R. C. Young, *Semin. Oncol.*, 2000, **27**, 8–10.
24 B. H. Long and C. R. Fairchild, *Cancer Res.*, 1994, **54**, 4355–4361.
25 S. Radulescu, R. A. Ridgway, P. Appleton, K. Kroboth, S. Patel, J. Woodgett, S. Taylor, I. S. Nathke and O. J. Sansom, *Oncogene*, 2010, **29**, 6418–27.
26 X. Wang, L. Pan, N. Mao, L. Sun, X. Qin and J. Yin, *Cancer Cell Int.*, 2013, **13**, 77.
27 X. Xiong, M. Sui, W. Fan and A. S. Kraft, *Cancer Biol. Ther.*, 2007, **6**, 1067–73.
28 K. Torres and S. B. Horwitz, *Cancer Res.*, 1998, **58**, 3620–3626.
29 C.-H. Shu, W. K. Yang, Y.-L. Shih, M.-L. Kuo and T.-S. Huang, *Apoptosis*, 1997, **2**, 463–470.
30 F. Bally, E. Ismailova, C. Brochon, C. A. Serra and G. Hadziioannou, *Macromolecules*, 2011, **44**, 7124–7131.
31 S. Bektas, M. Ciftci and Y. Yagci, *Macromolecules*, 2013, **46**, 6751–6757.
32 Z. Wei, J. Hao, S. Yuan, Y. Li, W. Juan, X. Sha and X. Fang, *Int. J. Pharm.*, 2009, **376**, 176–185.
33 J. Gong, M. Huo, J. Zhou, Y. Zhang, X. Peng, D. Yu, H. Zhang and J. Li, *Int. J. Pharm.*, 2009, **376**, 161–168.
34 L. Chang, L. Deng, W. Wang, Z. Lv, F. Hu, A. Dong and J. Zhang, *Biomacromolecules*, 2012, **13**, 3301–10.
35 O. Soga, C. F. van Nostrum, M. Fens, C. J. F. Rijcken, R. M. Schiffelers, G. Storm and W. E. Hennink, *J. Control. Release*, 2005, **103**, 341–53.
36 X. Zhang, J. K. Jackson and H. M. Burt, *Int. J. Pharm.*, 1996, **132**, 195–206.
37 O. Warburg, F. Wind and E. Negelein, *Klin. Wochenschr.*, 1926, **5**, 829–832.
38 A. Strambi and A. De Milito, in *Tumor Cell Metabolism*, Springer, 2015, pp. 173–196.
39 S. dos Santos, B. Medronho, T. dos Santos and F. E. Antunes, in *Drug Delivery Systems: Advanced Technologies Potentially Applicable in Personalised Treatment*, Springer, 2013, pp. 35–85.
40 J. P. Xu, J. Ji, W.-D. Chen and J. C. Shen, in *Key Engineering Materials*, 2005, vol. 288-289, pp. 465–468.
41 H. Liu, K. Miao, G. Zhao, C. Li and Y. Zhao, *Polym. Chem.*, 2014, **5**, 3071.
42 G. C. Das, D. Holiday, R. Gallardo and C. Haas, *Cancer Lett.*, 2001, **165**, 147–53.

TOC

Paclitaxel

Drug Loading

PMMA-*b*-PHEMA

Paclitaxel Loaded
PMMA-*b*-PHEMA

CONTROLLED
DRUG RELEASE

A549 Lung Cell Carcinoma